Electronic Supplementary Material (ESI) for ChemComm.

Controlling Molecular Shuttling in a Rotaxane with Weak Ring Recognition Sites

Nina Bukthiiarova,[a,b] Alberto Credi,*[,a,b] Stefano Corra*[,a,b]

[(a)] CLAN-Center for Light Activated Nanostructures, Istituto per la Sintesi Organica e Fotoreattività, CNR area della ricerca Bologna, via Gobetti, 101, 40129, Bologna, Italy.

[(b)] Dipartimento di Chimica Industriale "Toso-Montanari", Alma Mater Studiorum - Università di Bologna, viale del Risorgimento, 4, 40136 Bologna, Italy.

E-mail: stefano.corra@unibo.it, alberto.credi@unibo.it

SUPPLEMENTARY INFORMATION

1. Materials and methods

General materials. All reagents and chemicals were purchased from Sigma-Aldrich or VWR international and used as received unless otherwise stated. Flash column chromatography was performed using Sigma Aldrich Silica 40 (230-400 mesh size or 40-63 μm) as the stationary phase. Size exclusion chromatography was performed using Biorad Biobeads SX-3 as the stationary phase. Thin layer chromatography was performed on TLC Silica gel 60 F254 coated aluminum plates from Merck.

NMR Spectroscopy. NMR spectra were recorded on an Agilent DD2 spectrometer operating at 500 MHz. Chemical shifts are quoted in parts per million (*ppm*) relative to tetramethylsilane using the residual solvent peak as a reference standard and all coupling constants (*J*) are expressed in Hertz (Hz).

Mass spectrometry. High resolution mass spectrometry (HRMS) measurements were performed on a Waters Xevo G2-XS instrument equipped with an ESI source and a Q-TOF ion analyzer.

2. Synthetic procedures

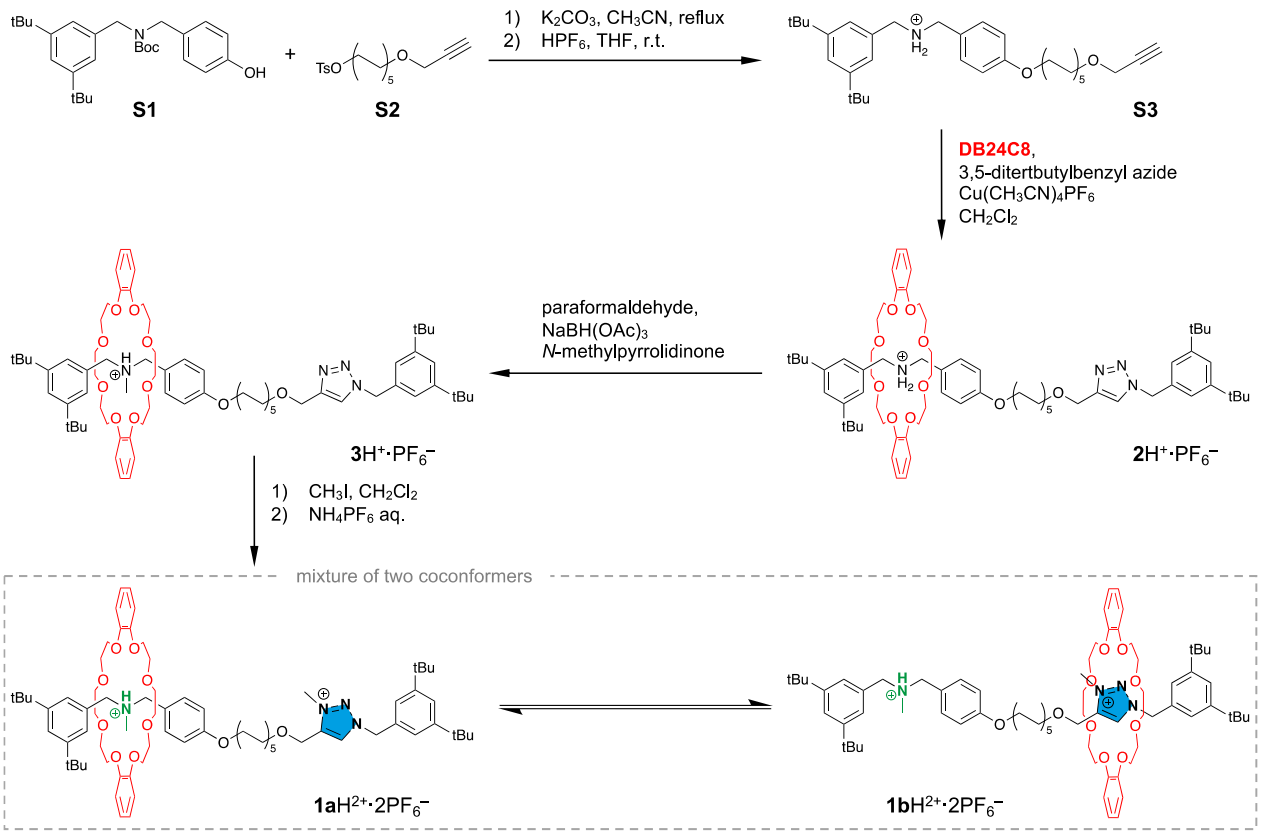

Scheme S1. Synthetic route for the preparation of rotaxanes **1a**H^{2+} and **1b**H^{2+}.

Compounds **S1** and **S2** were prepared according to previously reported procedures.[1,2] Analytical data were in line with those reported in literature. Compound S3 was prepared adapting a previously reported protocol.[1]

S3

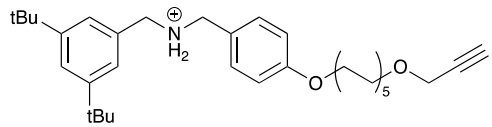

Compounds **S1** (2.5 g, 6 mmol) and **S2** (2.5 g, 6.6 mmol) and Cs_2CO_3 (5.6 g, 18 mmol) were suspended in dry MeCN (50 mL) under a nitrogen atmosphere. The reaction mixture was refluxed overnight under vigorous stirring. The mixture was concentrated, suspended in diethyl ether (200 mL) and washed with water (3 x 200 mL). The crude product was purified by flash chromatography (SiO_2, hexane/ethyl acetate 9:1) to afford the N-Boc protected intermediate as a yellow oil (2.68 g, 4.3 mmol, 70%).

^{1}H NMR (500 MHz, $CDCl_3$, 298 K) *δ (ppm)* 7.32 (s, 1H), 7.19 – 7.00 (m, 4H), 6.84 (d, J = 8.3 Hz, 2H), 4.32 (m, 4H), 4.14 (d, J = 2.4 Hz, 2H), 3.94 (t, J = 6.6 Hz, 2H), 2.42 (t, J = 2.4 Hz, 1H), 1.78 (t, J = 7.4 Hz, 2H), 1.65 – 1.22 (m, 14H), 1.31 (s, 18H).

A portion of the intermediate (1.5 g, 2.4 mmol) was then dissolved in dioxane/HCl conc. (2:1 v/v) and stirred for 1h. The volatiles were removed under vacuum, and the mixture was redissolved in CH_2Cl_2. Saturated aqueous solution of NH_4PF_6 was added and the biphasic mixture was stirred overnight. Layers were separated and the organic layer was washed with aqueous NH_4PF_6 (1 x 50 mL) and water (3 x 100 mL), and concentrated to afford the product (800 mg, 1.2 mmol, 50%) as a yellow oil which was used in crude purity.

2$H^+ \cdot PF_6^-$

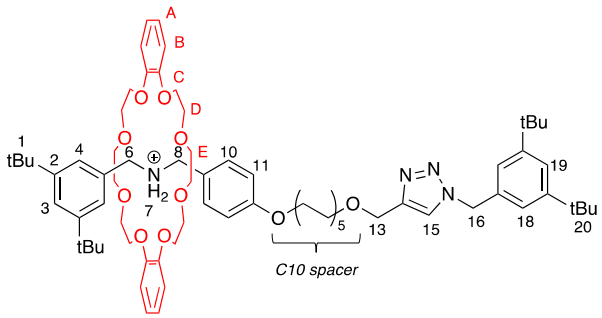

S3 (800 mg, 1.2 mmol), DB24C8 (1.08 g, 2.4 mmol), and 3,5-di(tertbutyl)benzyl azide (470 mg, 2 mmol) were dissolved in CH_2Cl_2 (10 mL). The solution was stirred for 30 min to ensure complete formation of the complex. The mixture was degassed by nitrogen purging for 20 min, then $Cu(CH_3CN)_4$ (450 mg, 1.2 mmol) was added and the reaction was stirred overnight under a nitrogen atmosphere.

The vessel was opened to air and an aqueous solution of EDTA (1 M, 10 mL) was added. The organic layer was washed further with aqueous EDTA (1 M, 3 x 50 mL) and water (3 x 50 mL). The combined organic layers were dried over $MgSO_4$ and concentrated under vacuum. The crude product was purified by size-exclusion chromatography (Biobeads SX-3, CH_2Cl_2) to afford the [2]rotaxane **2**$H^+ \cdot PF_6^-$ as a colourless foam (600 mg, 0.44 mmol, 40%).

^{1}H NMR (500 MHz, CD_2Cl_2, 298 K) *δ (ppm)* 7.49 (s, 2H, H_7), 7.46 (s, 1H, H_{15}), 7.42 (d, J = 1.9 Hz, 1H, H_{19}), 7.40 (d, J = 2.0 Hz, 1H, H_3), 7.30 (d, J = 1.8 Hz, 2H, H_4), 7.11 (d, J = 1.8 Hz, 2H, H_{18}), 7.08 (d, J = 8.4 Hz, 2H, H_{10}), 6.93 – 6.86 (m, 8H, H_A), 6.83 – 6.76 (m, 8H, H_B), 6.50 (d, J = 8.4 Hz, 2H, H_{11}), 5.47 (s, 2H, H_{16}), 4.75 – 4.69 (m, 2H, H_8), 4.53 (s, 2H, H_{13}), 4.52 – 4.48 (m, 2H, H_6), 4.14 – 4.05 (m, 8H, H_C), 3.83 – 3.68 (m, 10H, H_C +*C10 spacer*), 3.63 – 3.53 (m, 4H, H_E), 3.50 – 3.42 (m, 6H, H_E + *C10 spacer*), 1.71 (p, J = 6.8 Hz, 2H, *C10 spacer*), 1.53 (s, 6H, *C10 spacer*), 1.42 (s, 8H, *C10 spacer*), 1.29 (s, 18H, H_{20}), 1.20 (s, 18H, H_1). **^{13}C NMR (126 MHz, CD_2Cl_2, 298 K)** *δ (ppm)* 152.0, 147.9, 131.1, 124.0, 122.8, 122.0, 114.5, 112.9, 71.0, 70.6, 68.4, 64.5, 35.2, 31.5, 30.1, 29.9, 29.8. **HRMS (ESI+)** *m/z* calculated for $C_{74}H_{109}N_4O_{10}^+$ $[M]^+$ 1213.8143; found: 1213.8143.

3$H^+ \cdot PF_6^-$

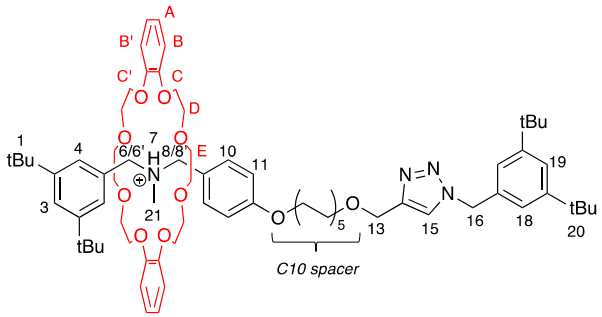

In a screw-capped vessel, under a nitrogen atmosphere, rotaxane **2**$H^+ \cdot PF_6^-$ (300 mg, 0.22 mmol, 1 equiv.), paraformaldehyde (20 equiv.), and $NaBH(OAc)_3$ (20 equiv.) were dissolved in N-methyl-2-pyrrolidone (2 mL) and the reaction mixture was stirred overnight at 70°C. The mixture was allowed to cool to room temperature and then precipitated by addition of water (100 mL). The white solid was filtered and washed with water. The solid was dissolved in EtOAc and washed with aqueous NH_4PF_6 (3 x 50 mL) and with H_2O (3 x 50 mL). The combined organic layers were dried over $MgSO_4$, concentrated under vacuum, and purified by size-exclusion chromatography (Biobeads SX-3, CH_2Cl_2) to afford **3**$H^+ \cdot PF_6^-$ as a white foam (230 mg, 0.17 mmol, 75%).

^{1}H NMR (500 MHz, CD_2Cl_2, 298 K) *δ (ppm)* 7.59 (s, 1H, H_7), 7.51 (d, *J* = 8.6 Hz, 2H, H_{10}), 7.49 – 7.45 (m, 2H, H_3 + H_{15}), 7.42 (t, J = 2.0 Hz, 1H, H_{19}), 7.25 (dd, J = 1.8, 0.9 Hz, 2H, H_4), 7.12 (dd, *J* = 1.8, 0.9 Hz, 2H, H_{18}), 6.93 – 6.87 (m, 8H, H_A), 6.87 – 6.75 (m, 8H, H_B), 6.51 (d, *J* = 8.4 Hz, 2H, H_{11}), 5.47 (s, 2H, H_{16}), 5.19 – 5.10 (m, 2H, $H_{8/8'}$), 4.60 – 4.54 (m, 1H, H_6), 4.53 (s, 2H, H_{13}), 4.30 – 4.20 (m, 3H, $H_{6'}$ + H_C), 4.17 – 4.09 (m, 6H, H_C), 3.89 – 3.57 (m, 18H, H_D + H_E + *C10 spacer*), 3.45 (t, *J* = 6.7 Hz, 2H, *C10 spacer*), 2.95 (d, *J* = 5.3 Hz, 3H, H_{21}), 1.66 (p, *J* = 6.7 Hz, 2H, *C10 spacer*), 1.59 – 1.50 (m, 6H, *C10 spacer*), 1.44 – 1.24 (m, 44H, H_1 + H_{20} + *C10 spacer*). **^{13}C NMR (126 MHz, CD_2Cl_2, 298 K)** *δ (ppm)* 160.2, 152.4, 152.2, 147.8, 147.6, 146.0, 134.6, 133.7, 130.4, 125.3, 124.2, 123.1, 122.9, 122.8, 122.7, 121.7, 121.6, 114.1, 112.2, 112.1, 72.2, 72.1, 71.3, 71.0, 70.9, 68.5, 68.2, 68.1, 64.5, 61.5, 61.4, 55.0, 39.9, 35.2, 35.1, 31.6, 31.5, 31.4, 30.1, 29.9, 29.8, 29.5, 26.5, 26.4. **HRMS (ESI+)** *m/z* calculated for $C_{75}H_{111}N_4O_{10}^+$ $[M]^+$ 1227.8301; found: 1227.8301.

1$H^{2+} \cdot 2PF_6^-$

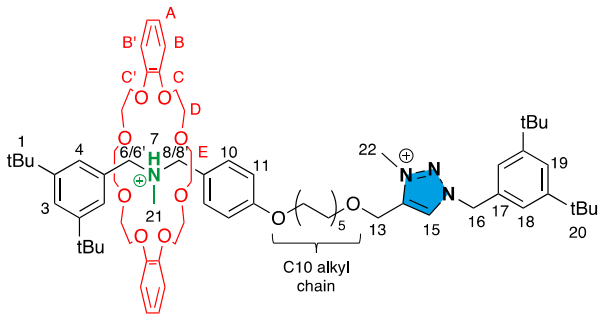

Rotaxane **3**$H^+ \cdot PF_6^-$ (210 mg, 0.15 mmol) was dissolved in the minimum amount of CH_3I (5 mL) and the solution was stirred for three days. Volatiles were removed under vacuum, the residue was dissolved in CH_2Cl_2 and washed with aqueous NH_4PF_6 (3 x 50 mL). The organic layer was

dried over $MgSO_4$ and concentrated under vacuum. The crude product was purified by size-exclusion chromatography (Biobeads SX-3, CH_2Cl_2) to afford **1**$H^{2+}\cdot 2PF_6^-$ as a glassy solid (173 mg, 0.11 mmol, 75%). The compound exists as a mixture of two co-conformers in a 95:5 relative ratio in CD_2Cl_2.

^{1}H NMR (500 MHz, CD_2Cl_2, 298 K, major coconformer "a") *δ (ppm)* 8.19 (s, 1H, H_{15}), 7.60 (s, 1H, H_7), 7.54 (t, *J* = 1.8 Hz, 1H, H_3), 7.51 (d, *J* = 8.1 Hz, 2H, H_{10}), 7.49 – 7.47 (m, 1H, H_{19}), 7.30 (s, 2H, H_4), 7.25 (d, J = 1.7 Hz, 2H, H_{18}), 6.93 – 6.86 (m, 8H, H_A), 6.84 – 6.77 (m, 8H, $H_{B/B'}$), 6.51 (d, J = 8.1 Hz, 2H, H_{11}), 5.65 (s, 2H, H_{16}), 5.23 – 5.04 (m, 2H, $H_{8/8'}$), 4.68 (s, 2H, H_{13}), 4.62 – 4.49 (m, 1H, $H_{6'}$), 4.32 – 4.18 (m, 6H, H_6 + H_{22} + $H_{C/C'}$), 4.17 – 4.07 (m, 6H, $H_{C/C'}$), 3.91 – 3.48 (m, 20H, H_D + H_E + *C10 spacer*), 2.94 (s, 2H, H21), 1.73 – 1.48 (m, 8H), 1.45 – 1.22 (m, 44H, H_1 + H_{20} + *C10 spacer*). **^{13}C NMR (126 MHz, CD_2Cl_2, 298 K, major coconformer "a")** *δ (ppm)* 152.36, 147.77, 133.71, 125.34, 124.88, 124.24, 121.68, 121.60, 114.09, 112.14, 72.57, 72.10, 71.34, 70.88, 68.55, 68.25, 39.89, 35.29, 35.21, 31.55, 31.50, 31.42, 29.85, 29.81, 29.74, 29.69, 29.50, 26.32, 26.26. **HRMS (ESI+)** *m/z* calculated for $C_{76}H_{114}N_4O_{10}^+$ $[M]^{2+}$ 622.4346; found: 622.4346.

3. NMR characterization of rotaxane $3H^+ \cdot PF_6^-$

Upon methylation, the symmetry plane which contains the axle is lost, and several signals, which were enantiotopic in the sec-ammonium rotaxane, become diastereotopic.[3,4] In particular, the benzylic protons H_6 and H_8, split into three distinct sets of resonances, displaying scalar coupling, which correspond to the diastereotopic protons $H_6/H_{6'}$ and $H_8/H_{8'}$ (Figure S1b). Because of the constrains of the mechanical bond, which does not allow the DB24C8 ring to rotate about the axle contained by the symmetry plane of the axle, the protons of the macrocycle also become diastereotopic. This is particularly evident for protons H_B and H_C which display two sets of resonances ($H_B/H_{B'}$ and $H_C/H_{C'}$), *syn* and *anti* with respect to the NMe group (Figure S1b and Figure S2). Similar stereochemical considerations can be done for the final rotaxane **1a**$H^+ \cdot PF_6^-$. These effects are not generally observed in the NMR spectra of tertiary ammonium salts because of the fast nitrogen inversion kinetics on the NMR timescale. However, pyramidal inversion in rotaxane **3**$H^+ \cdot PF_6^-$ is slow on the NMR timescale due to the presence of a hydrogen bond between the NH proton and the oxygen atoms of the DB24C8 ring which slows the kinetics of proton transfer.[5]

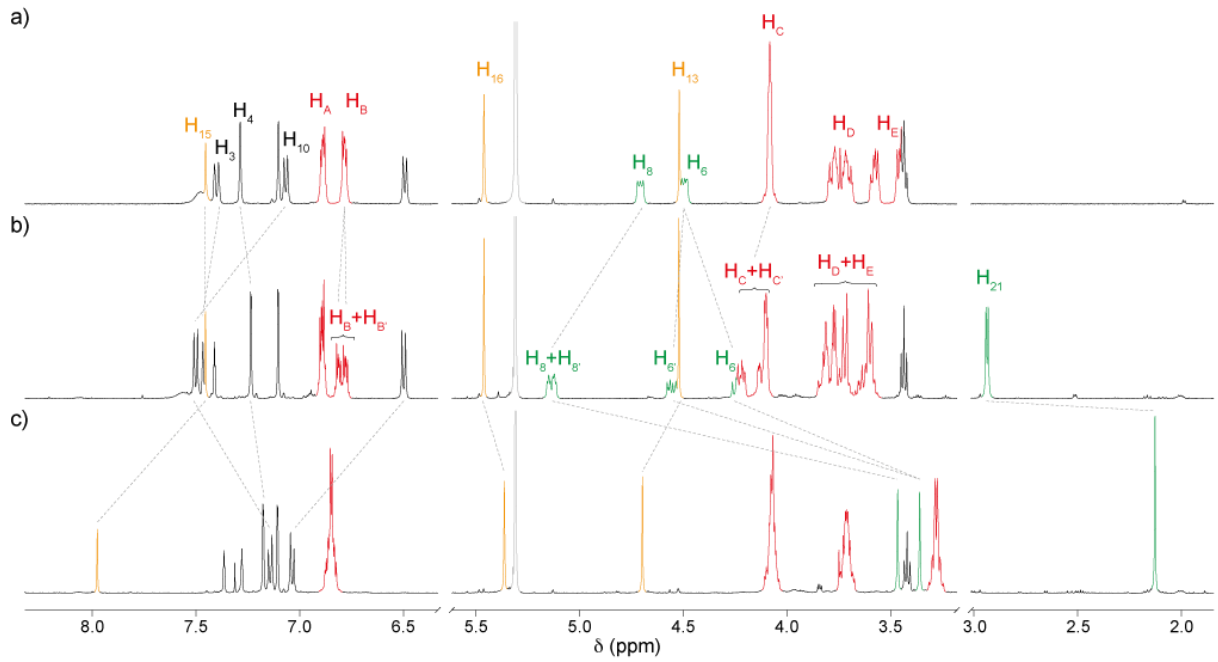

Figure S1. Partial ^{1}H NMR spectra (500 MHz, CD_2Cl_2, 298 K) of a) **2**$H^+ \cdot PF_6^-$, b) **3**$H^+ \cdot PF_6^-$, c) the same sample as in (b) after addition of resin-bound BEMP. The numbering and colour coding of significant proton signals is the same of scheme S1. The signal of the residual solvent is indicated in grey.

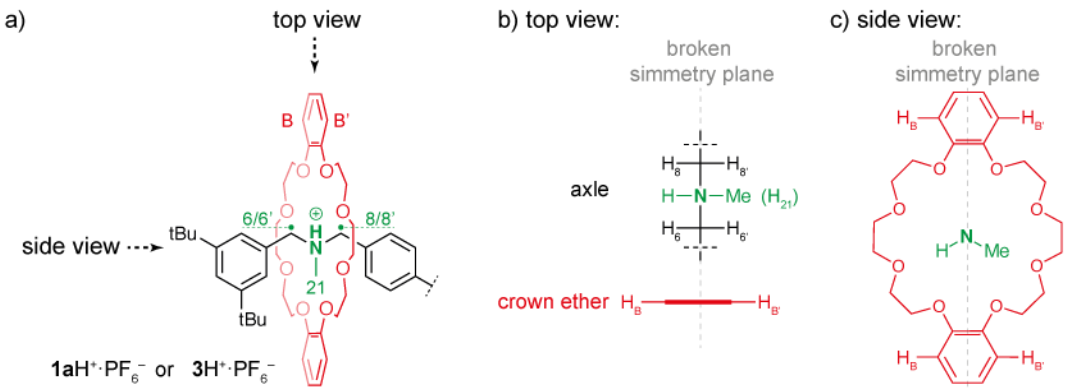

Figure S2. a) Projections of the encircled tertiary ammonium station in rotaxane **1a**$H^+ \cdot PF_6^-$ or **3**$H^+ \cdot PF_6^-$. b) Top view (fischer's projection) of the axle and DB24C8. c) Side view (along the axle) of DB24C8.

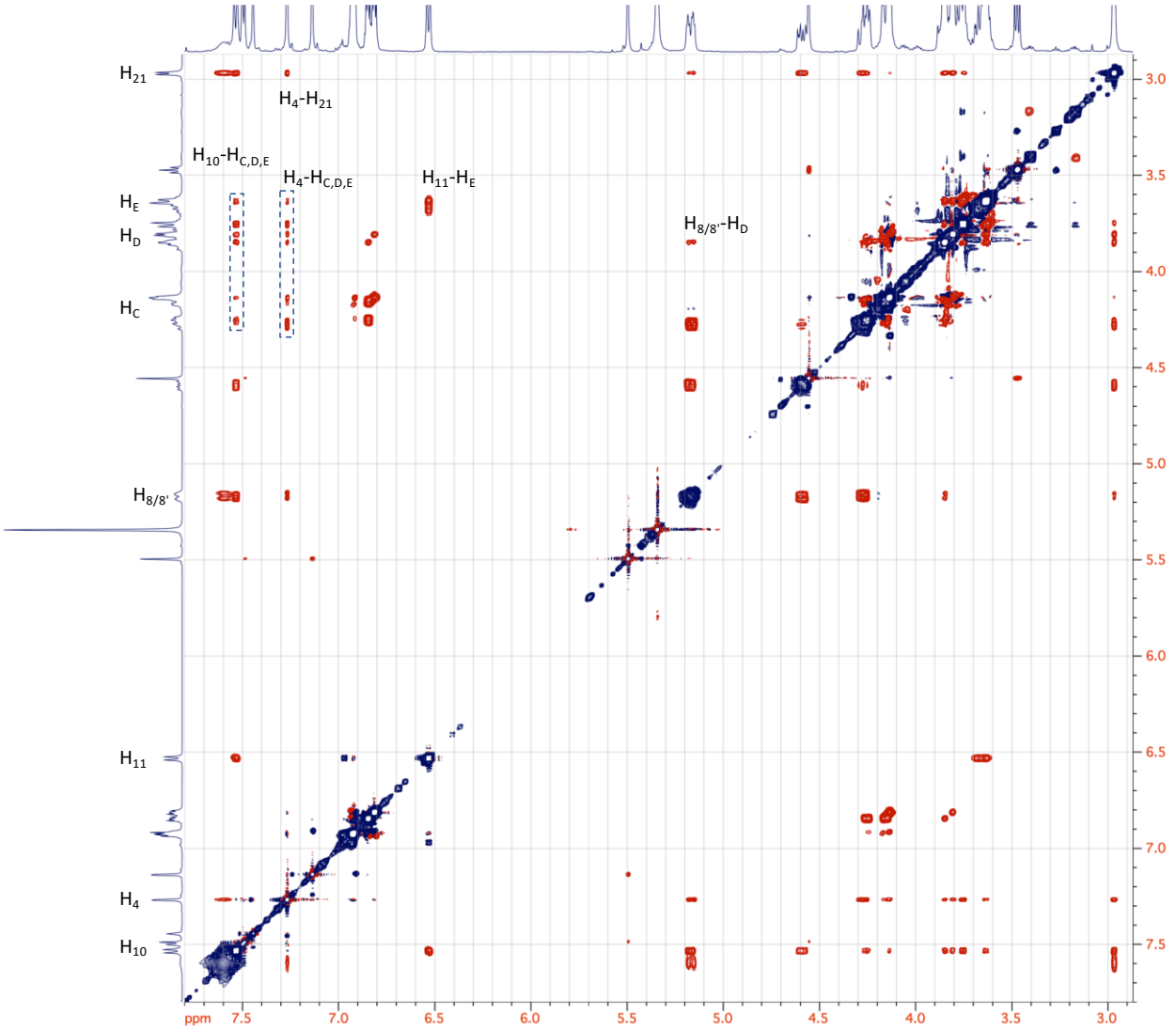

Figure S3. ROESY spectrum of **3**$H^+ \cdot PF_6^-$ (500 MHz, CD_2Cl_2, 298 K, t_{mix} 300 ms). Relevant NOE cross-peaks are indicated.

ROESY data (Figure S3) of rotaxane **3**$H^+ \cdot PF_6^-$ in CD_2Cl_2 indicate that the DB24C8 macrocycle is located to the ammonium-portion of the molecule but not directly bound to the *tert*-ammonium

cation, similarly to what is normally observed in the case in *sec*-ammonium rotaxanes. The ring, in fact, is shifted towards the flanking aromatic rings most likely to accommodate the bulky methyl group. Strong NOE cross-peaks are visible between H_{10} and the aliphatic signals of the DB24C8 ring (H_C, H_D, H_E). Considering the NOE interactions along with the variations in chemical shifts of protons associated with the dumbbell and ring components, it is reasonable that the aliphatic portion of DB24C8 interacts strongly with H_{10}, probably via H-bond. Conversely, $H_{6/6'}$ and $H_{8/8'}$, which typically are involved in H-bonding with the ring in *sec*-ammonium stations, display weaker ($H_{8/8'}$) or no ($H_{6/6'}$) NOE signals with aliphatic protons of the ring. Specifically, only the cross-peak between $H_{8/8'}$ and H_D could be detected clearly. Such a preferred conformation is also in line with downfield shift observed for H_{10} and H_3 ($\Delta\delta$ = 0.44 ppm and 0.07 ppm, respectively), while H_4 shifted upfield of 0.05 ppm (Figure S1b).

To test the operation of rotaxane **3**$H^+ \cdot PF_6^-$ as a pH-controlled molecular switch, resin-bound 2-tertbutylimino-2-diethylamino-1,3-dimethylperhydro-1,3,2-diazaphosphorine (BEMP) was added to a solution in CD_2Cl_2 (Figure S1c). Clean deprotonation of the ammonium station was achieved immediately, as evidenced by the upfield shift of H_{21} from 2.93 ppm to 2.13 ppm. Additionally, all the signals related to the triazole portion of the molecule (H_{13}, H_{15} and H_{16}.) exhibit large chemical shift variations. In particular, the sharp resonance at 7.98 ppm is associated with H_{15} in the complexed triazole.[6] The variation in chemical shift is also accompanied by the change in multiplicity, from a doublet to a singlet, due to the loss of scalar coupling with the NH proton. All diastereotopic signals resolved because of the slow N-inversion ($H_{6/6'}$, $H_{8/8'}$, $H_{B/B'}$ and $H_{C/C'}$) become isochronous again, indicating a fast process of nitrogen inversion of the uncomplexed tertiary amine on the NMR timescale.

4. Coconformational equilibria

4.2. Effect of the solvent

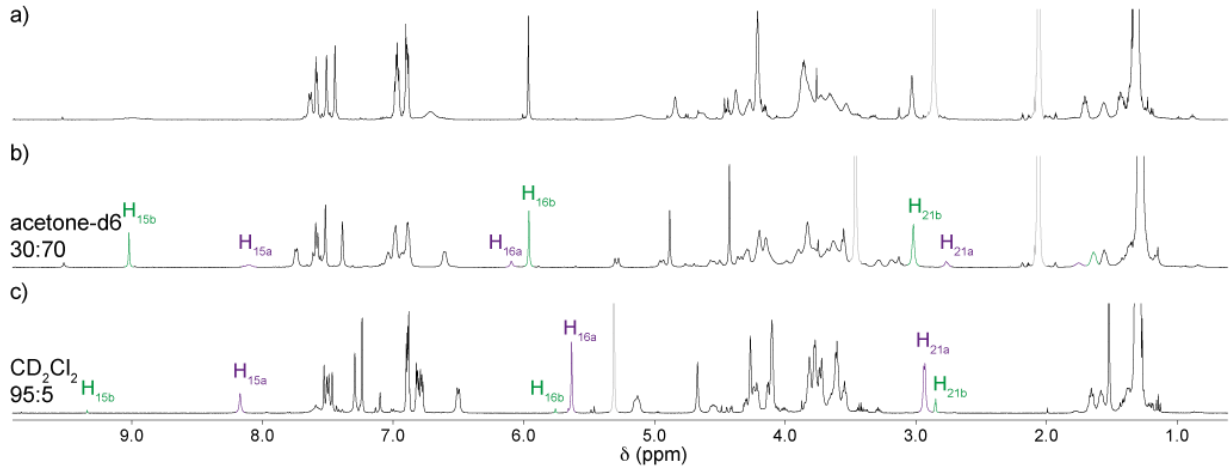

Figure S4. Partial ^{1}H NMR spectra (500 MHz) of a) **1**H^{2+}·2PF$_6^-$ in acetone-d$_6$ at 298 K, b) the same sample at 223 K showing slow exchange dynamics in the NMR timescale, c) **1**H^{2+}·2PF$_6^-$ in CD_2Cl_2 at 298 K. Diagnostic signals of coconformers **1a**H^{2+}·2PF$_6^-$ and **1b**H^{2+}·2PF$_6^-$ are highlighted in purple and green respectively. The relative molar ratio of the coconformers is indicated in panels (b) and (c) as **1a**H^{2+}:**1b**H^{2+}. Signals of the residual solvent and H_2O are indicated in grey.

4.2. Effect of the ion pairing

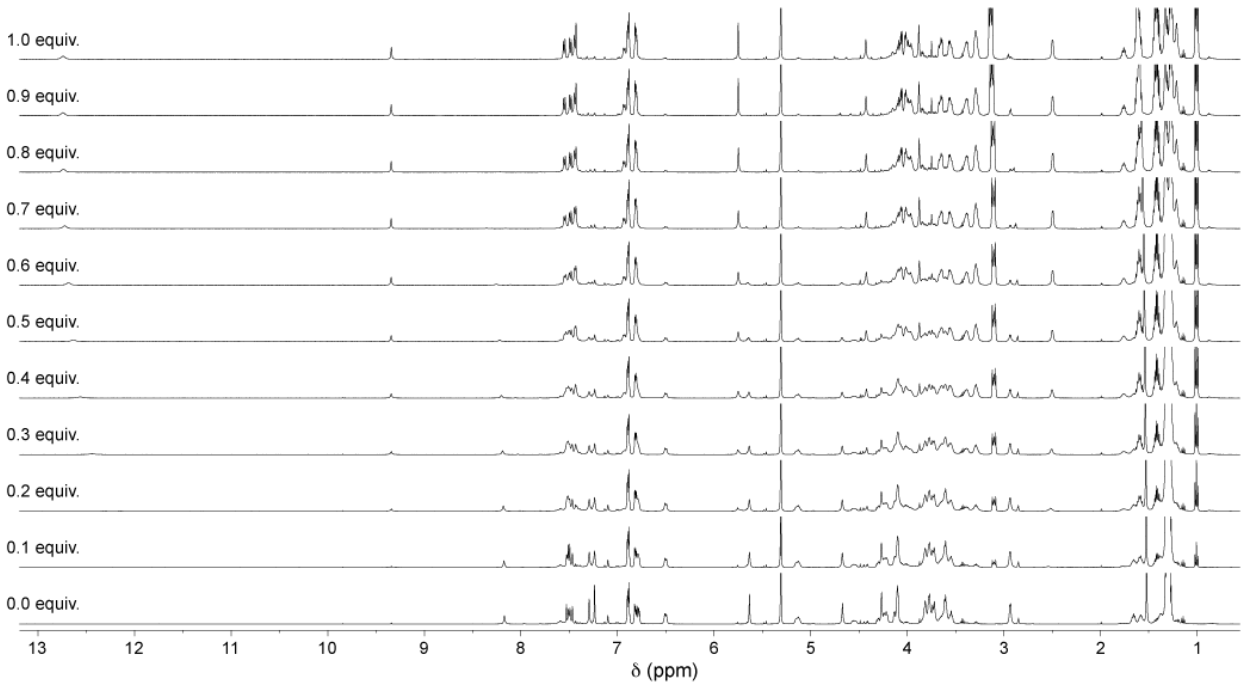

Figure S5. ^{1}H NMR spectra (500 MHz, CD_2Cl_2, 298 K) of **1**H^{2+}·2PF$_6^-$ upon titration with TBACl. The equivalents of TBACl added are reported on the left.

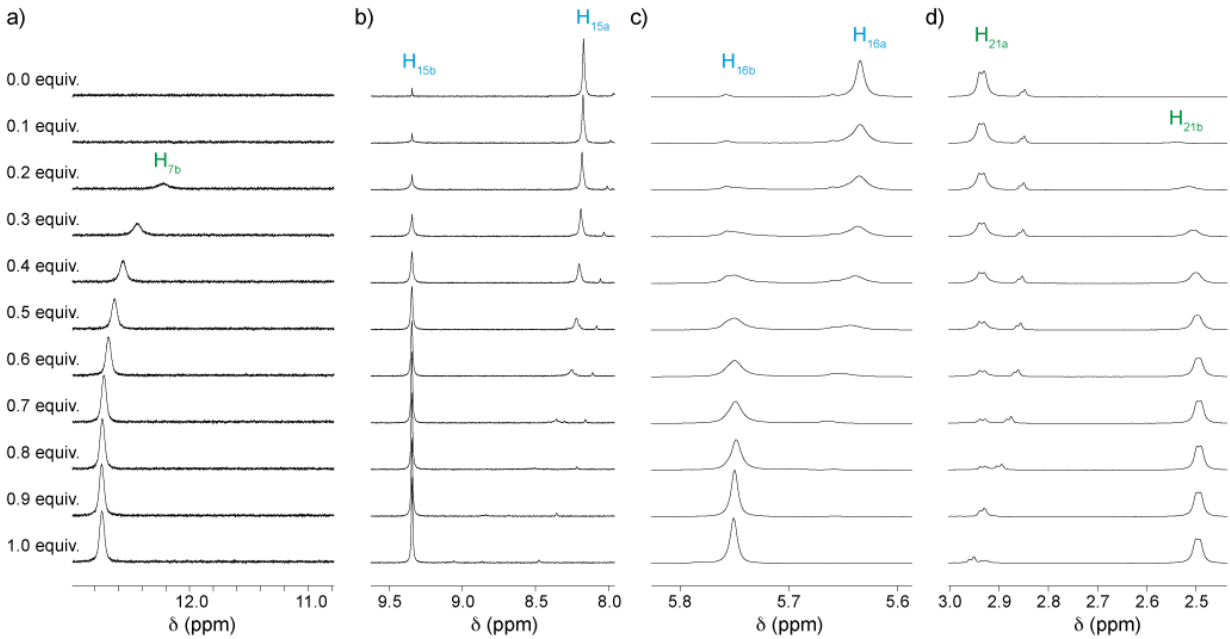

Figure S6. Partial ^{1}H NMR spectra (500 MHz, CD_2Cl_2, 298 K) of **1**$H^{2+}\cdot 2PF_6^-$ upon titration with TBACl in the regions of a) NH (H_7), b) triazolium (H_{15}), c) H_{16} and d) NMe (H_{21}) protons. The equivalents of TBACl added are reported on the left.

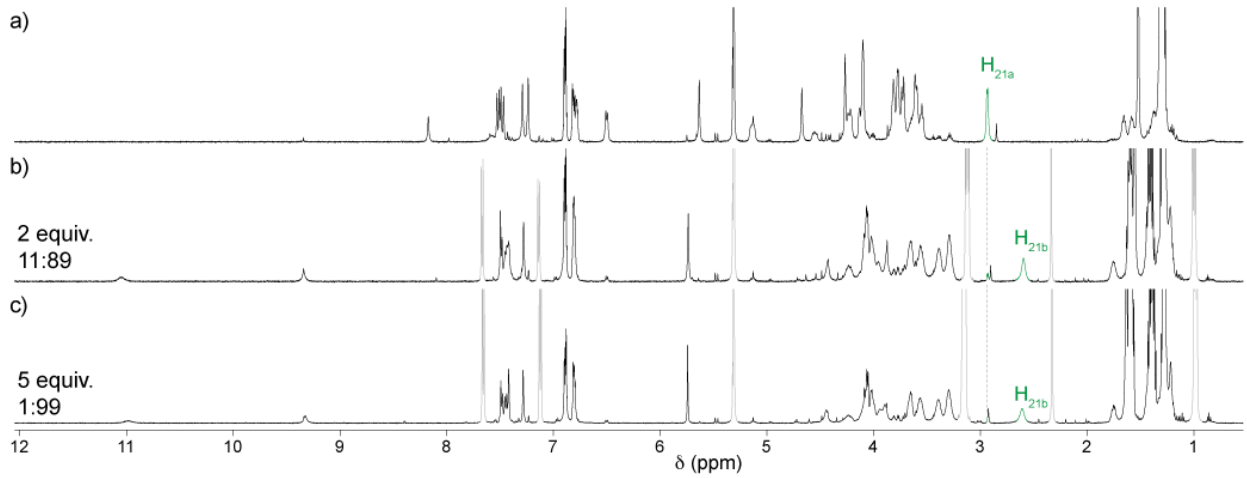

Figure S7. ^{1}H NMR spectra (500 MHz, CD_2Cl_2, 298 K) of **1**$H^{2+}\cdot 2PF_6^-$ at different amounts of TBAOTs. The equivalents of TBAOTs added are reported on the left along with the coconformers ratio **1a**H^{2+}:**1b**H^{2+}. Signals of the residual solvent and TBAOTs are indicated in grey.

*4.3 Deprotonation of **1**$H^{2+}\cdot 2PF_6^-$*

Rotaxane **1**$H^{2+}\cdot 2PF_6^-$ in CD_2Cl_2 was deprotonated *in situ* by adding resin-bound BEMP to deactivate the ammonium station. ^{1}H NMR spectra recorded after deprotonation showed the appearance of a singlet at 9.34 ppm confirming that rings quantitatively moved to the triazolium station. In figure S8 a comparison of rotaxanes **1**$H^{2+}\cdot 2Cl^-$ and deprotonated **1**$^{+}\cdot PF_6^-$ is shown to demonstrate the chloride induced ring shuttling.

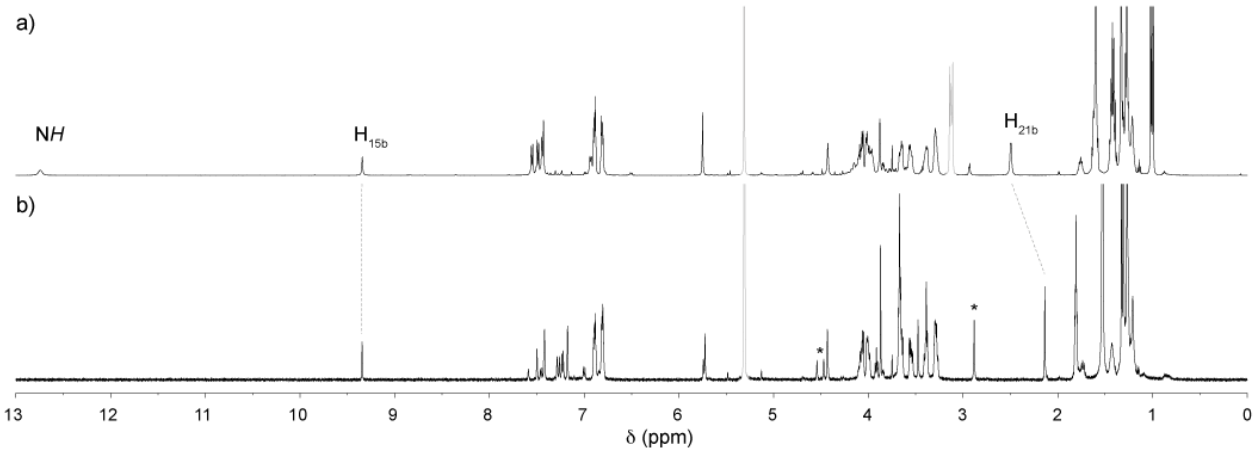

Figure S8. ^{1}H NMR spectra (500 MHz, CD_2Cl_2, 298 K) of **1**$H^{2+}\cdot 2Cl^-$ (a) and **1**$^{+}\cdot PF_6^-$ (b). Signals of the residual solvent and TBACl are indicated in grey. The signals marked with a * belong to an impurity which formed upon deprotonation.

4.4 Ring shuttling kinetics

To prove the chemical exchange between the two coconformers, induced by ring shuttling, exchange spectroscopy (EXSY) was used. The EXSY spectrum showed in Figure 3b of the manuscript was acquired on a solution of **1**$H^{2+}\cdot 2PF_6^-$ in CD_2Cl_2 where tetrabutylammonium chloride was added to reach a 50:50 relative population of the two coconformers ($K_{cc} \approx 1$) in order to maximize the signal-to-noise ratio for both coconformers.

The intermediate exchange on the NMR timescale between the coconformers observed in acetone was confirmed by variable temperature (VT) NMR. ^{1}H NMR spectra were acquired every 10 K in the range 223-303 K (Figure S9).

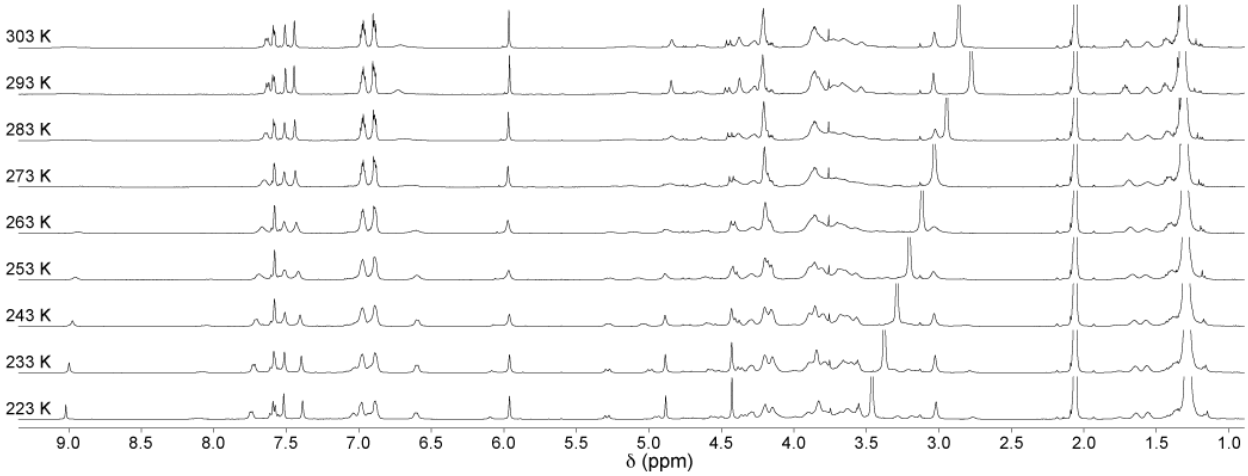

Figure S9. Variable temperature ^{1}H NMR spectra (500 MHz, acetone-d_6) of **1**$H^{2+}\cdot 2PF_6^-$.

5. NMR spectra

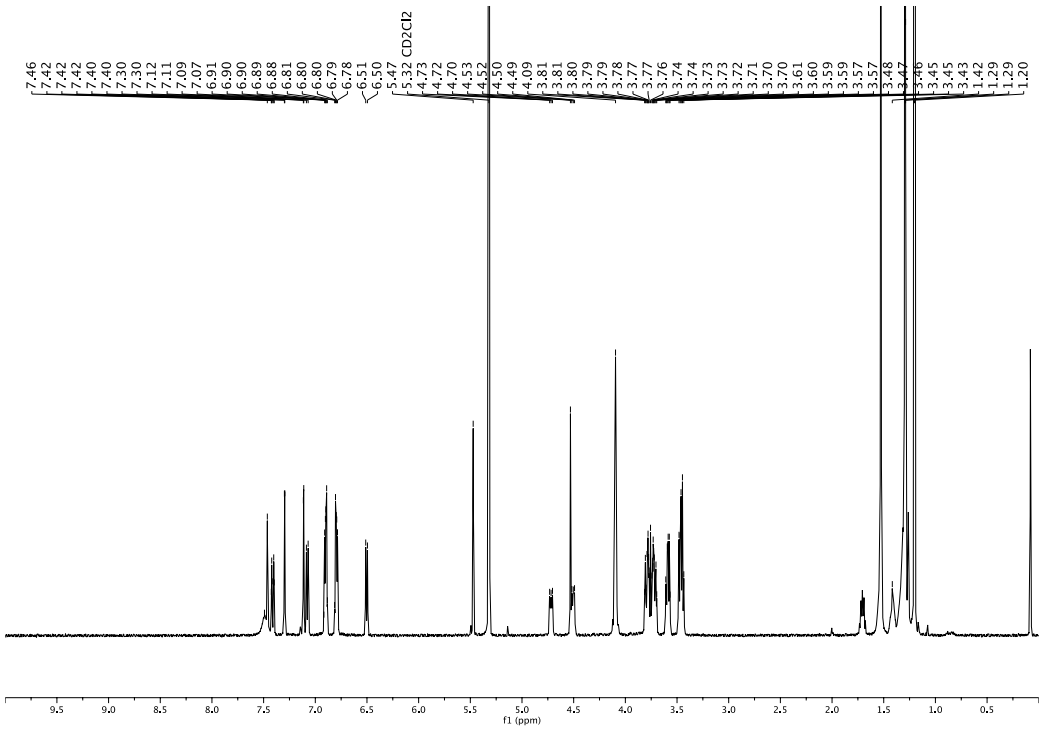

Figure S10. ^{1}H NMR spectrum of **2**H^{+}·PF$_{6}^{-}$ (500 MHz, CD_2Cl_2, 298 K).

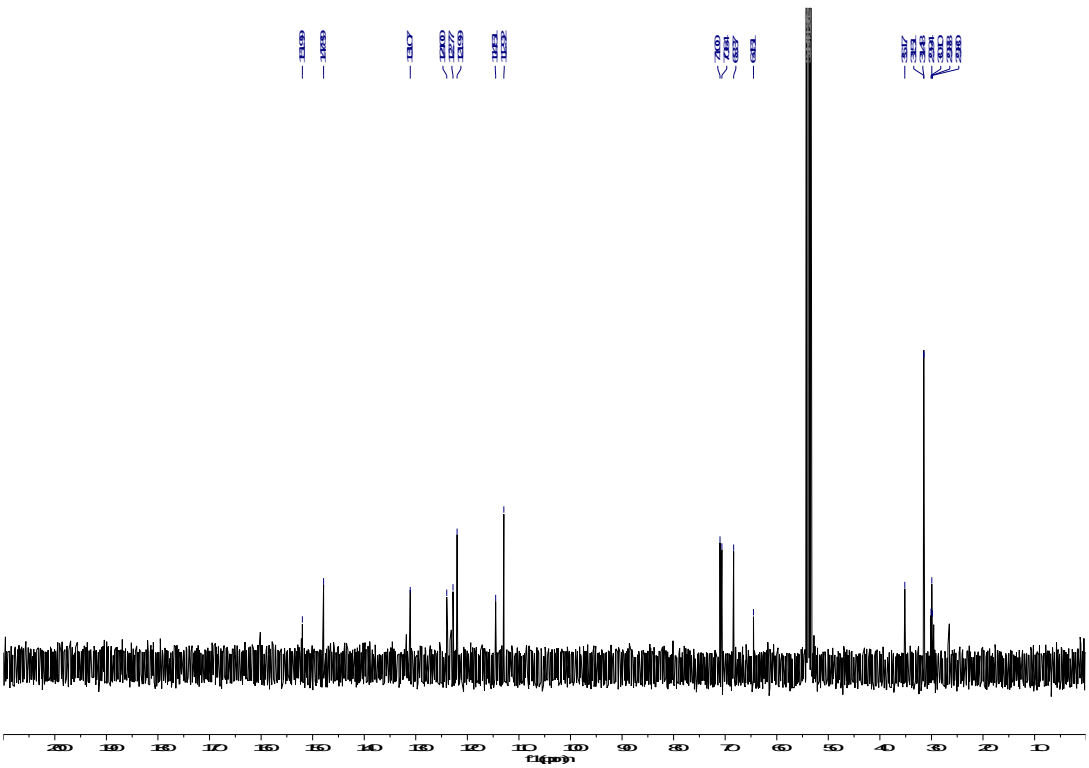

Figure S11. ^{13}C NMR spectrum of **2**H^{+}·PF$_{6}^{-}$ (125 MHz, CD_2Cl_2, 298 K).

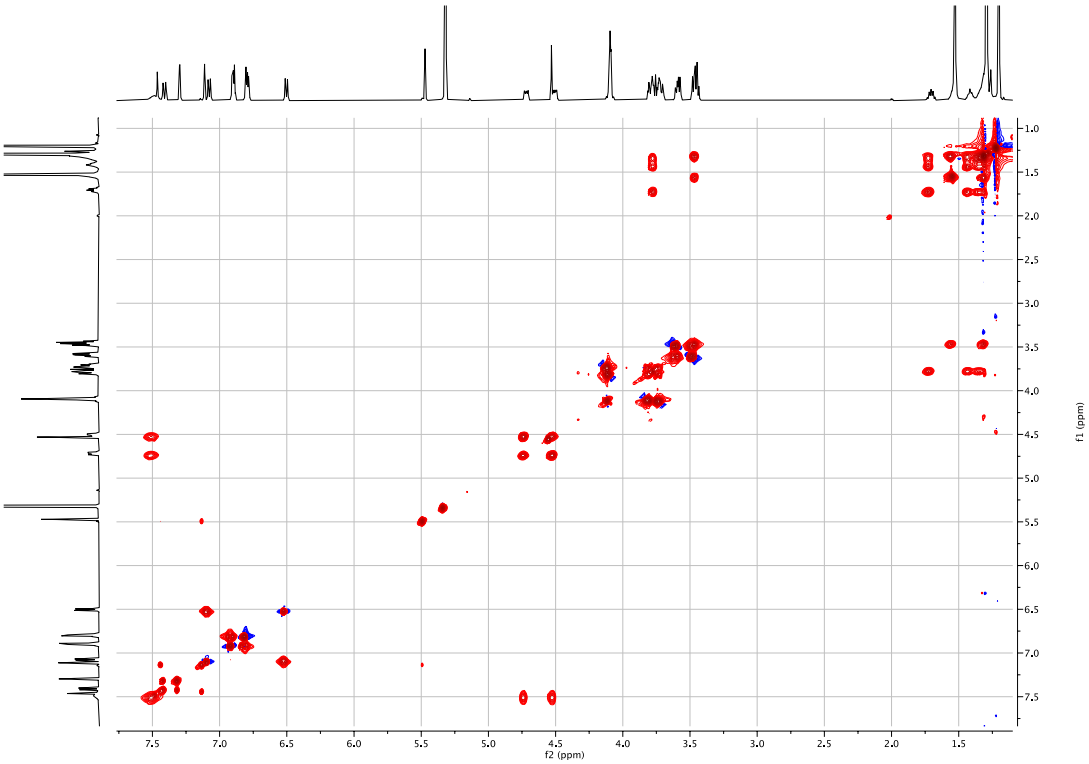

Figure S12. TOCSY spectrum of **2**$H^+ \cdot PF_6^-$ (500 MHz, CD_2Cl_2, 298 K, spinlock 80 ms).

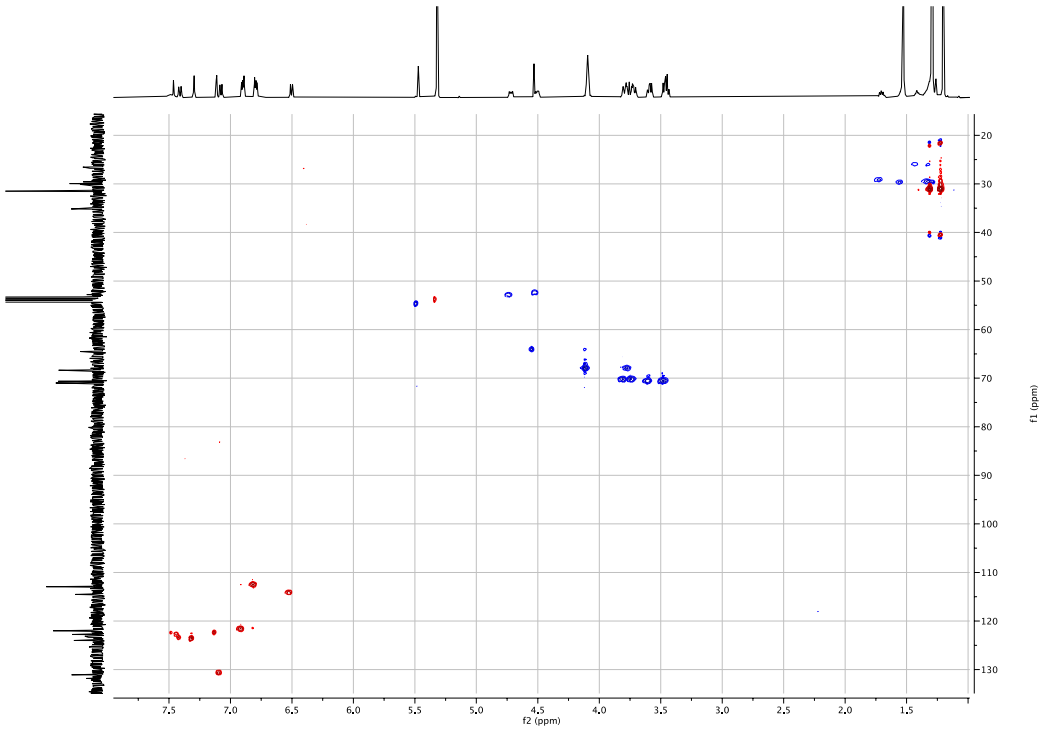

Figure S13. ^1H–^{13}C HSQC spectrum of **2**$H^+ \cdot PF_6^-$ (125 MHz, CD_2Cl_2, 298 K).

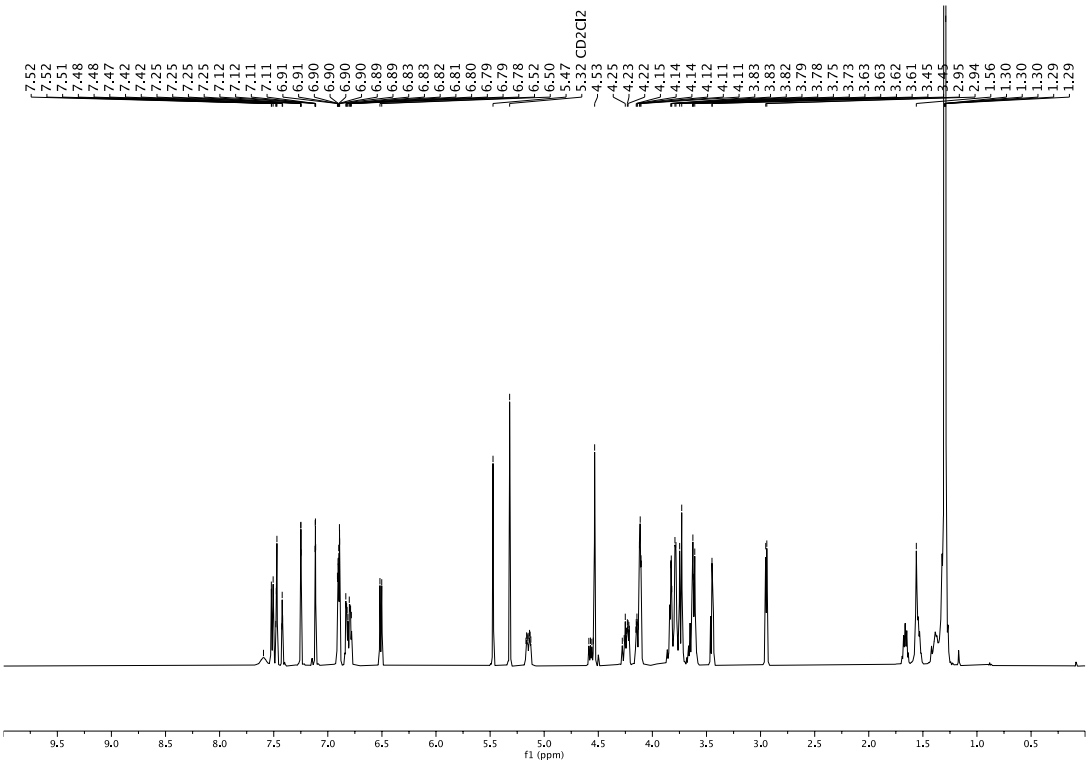

Figure S14. ^{1}H NMR spectrum of **3**$H^{+}\cdot PF_6^{-}$ (500 MHz, CD_2Cl_2, 298 K).

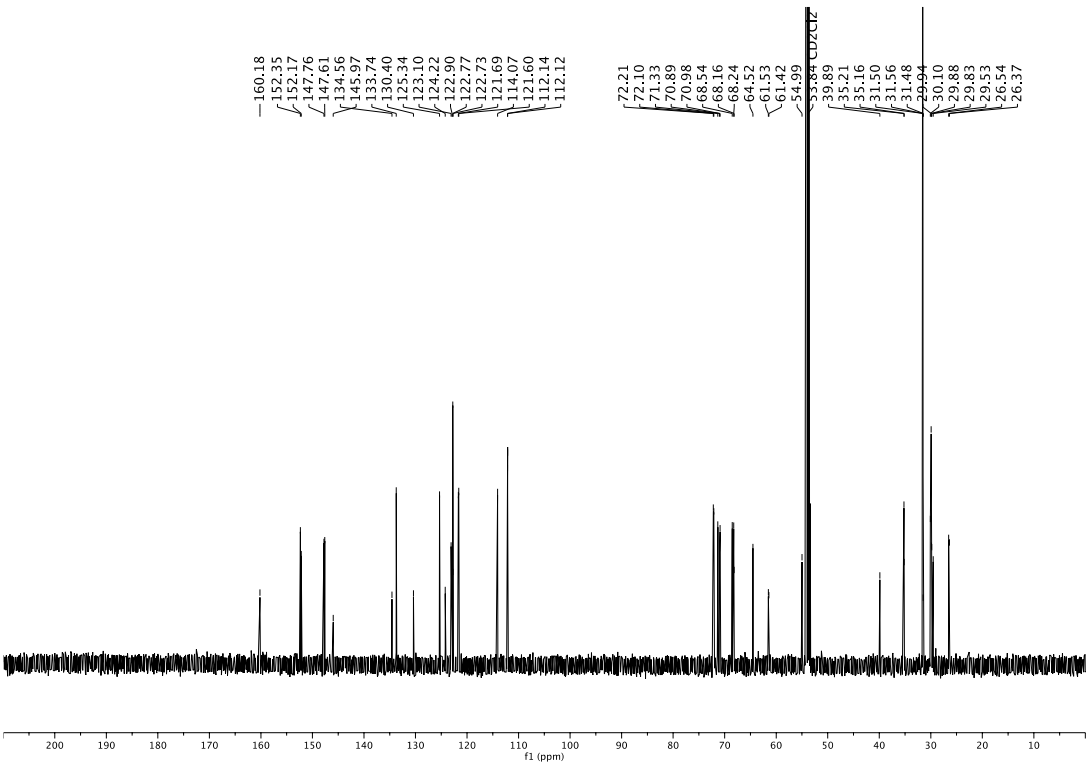

Figure S15. ^{13}C NMR spectrum of **3**$H^{+}\cdot PF_6^{-}$ (125 MHz, CD_2Cl_2, 298 K).

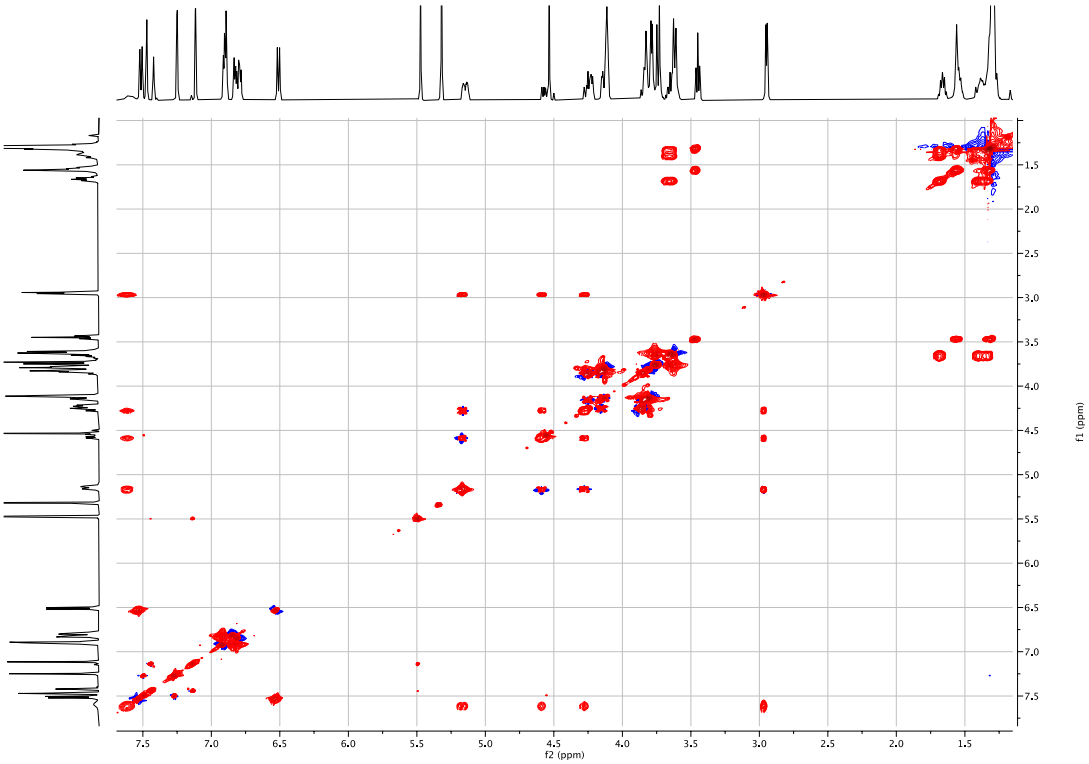

Figure S16. TOCSY spectrum of **3**H$^+$·PF_6^- (500 MHz, CD_2Cl_2, 298 K, spinlock 80 ms).

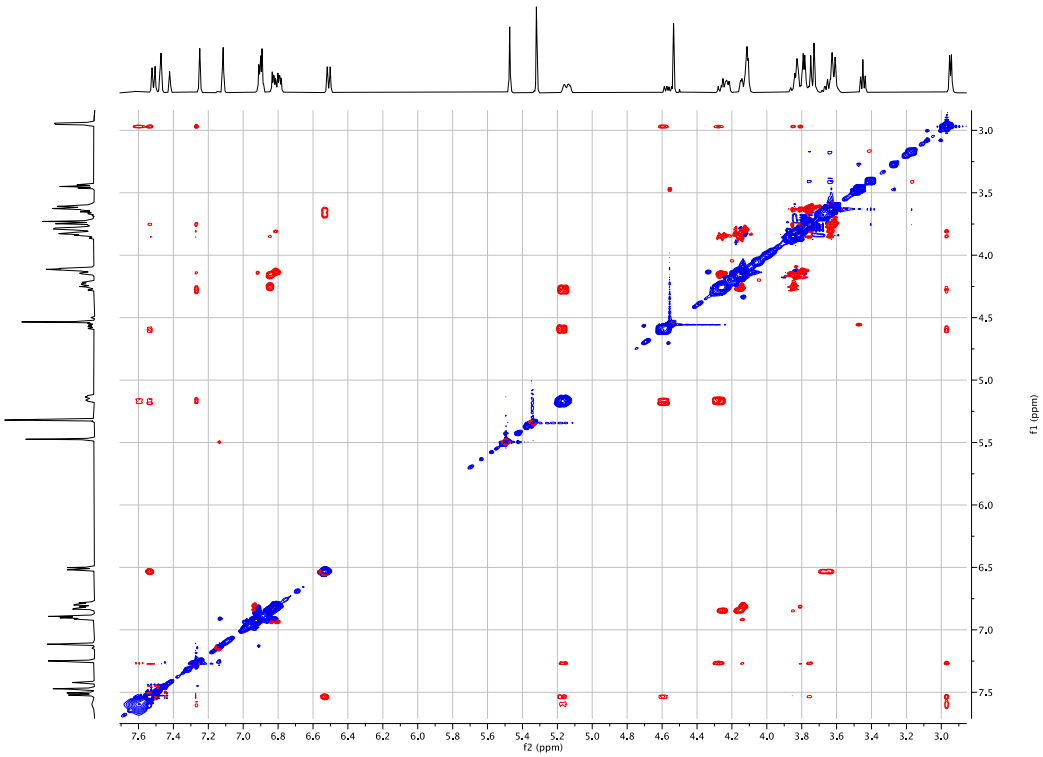

Figure S17. ROESY spectrum of **3**H$^+$·PF_6^- (500 MHz, CD_2Cl_2, 298 K, t_{mix} 300 ms).

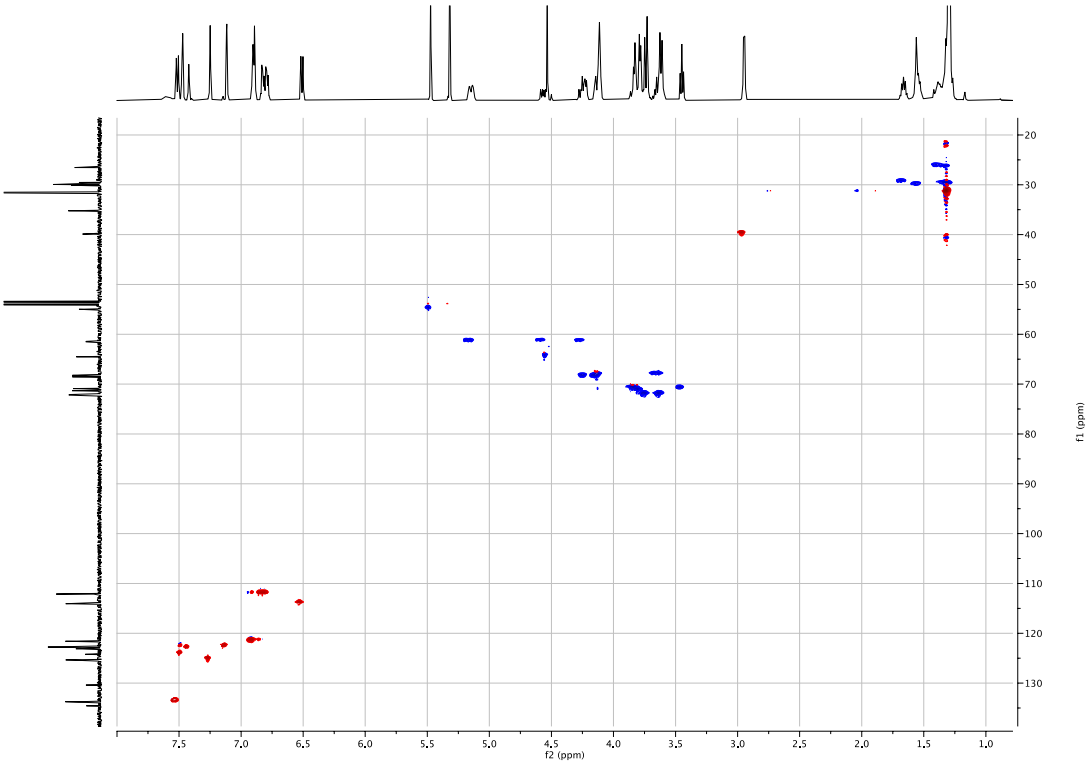

Figure S18. ^{1}H–^{13}C HSQC spectrum of **3**$H^{+}\cdot PF_6^{-}$ (125 MHz, CD_2Cl_2, 298 K).

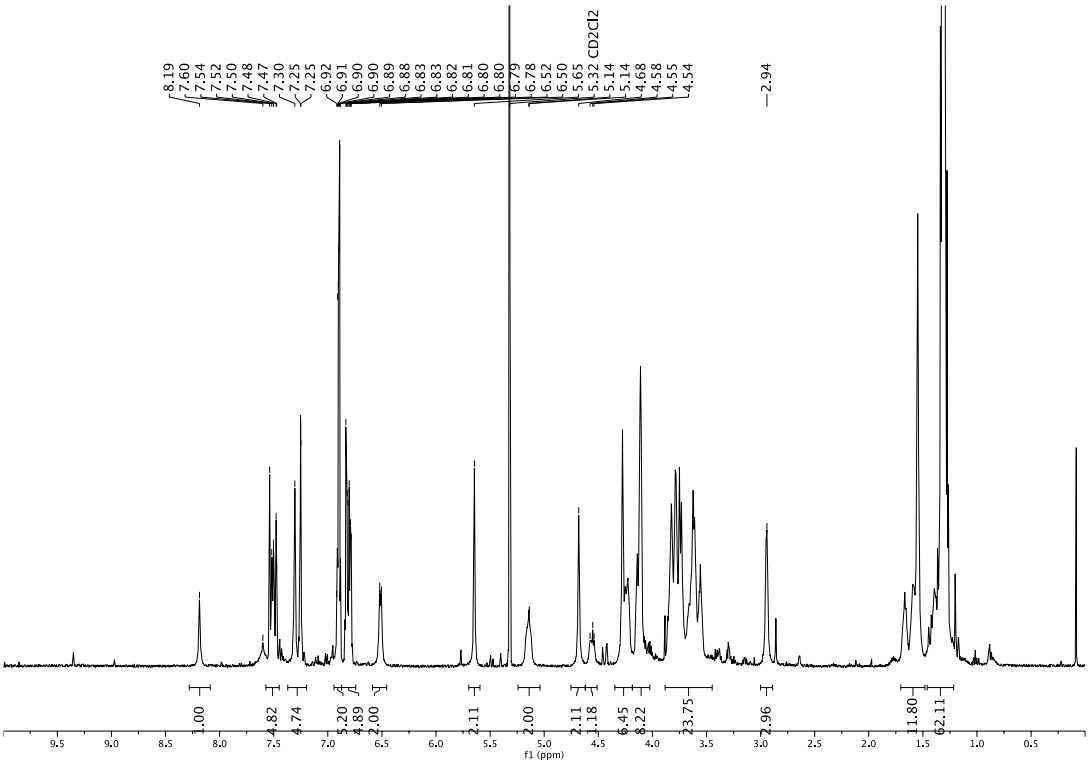

Figure S19. ^{1}H NMR spectrum of **1**$H^{2+}\cdot 2PF_6^-$ (500 MHz, CD_2Cl_2, 298 K).

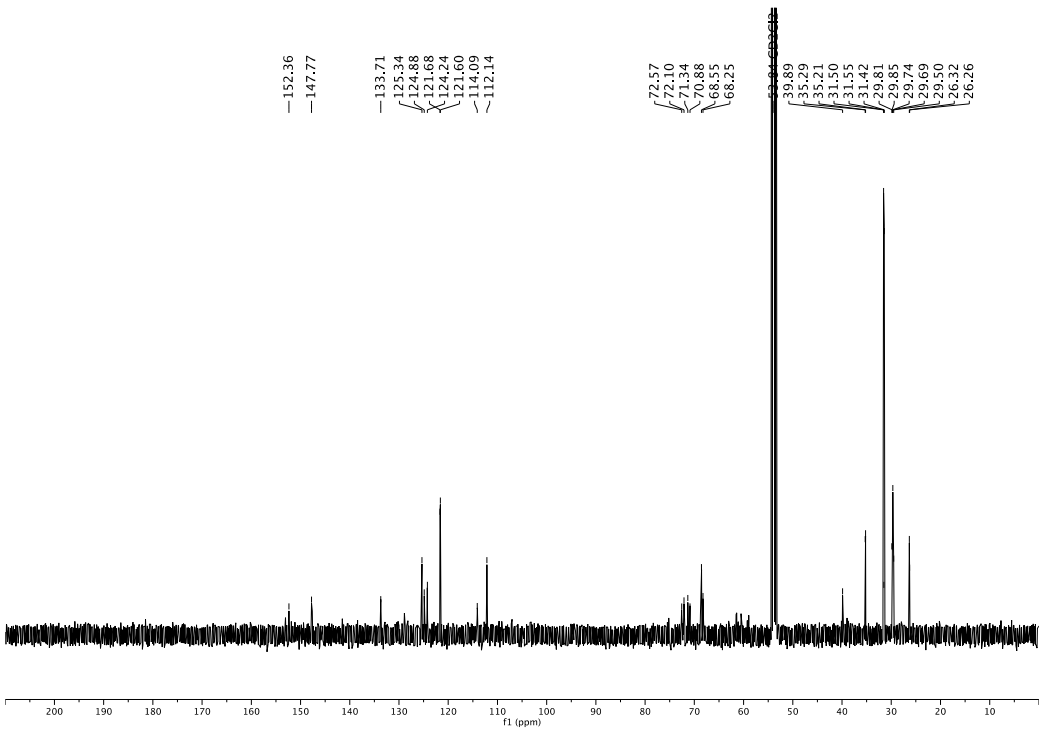

Figure S20. ^{13}C NMR spectrum of **1**$H^{+}\cdot PF_6^-$ (125 MHz, CD_2Cl_2, 298 K).

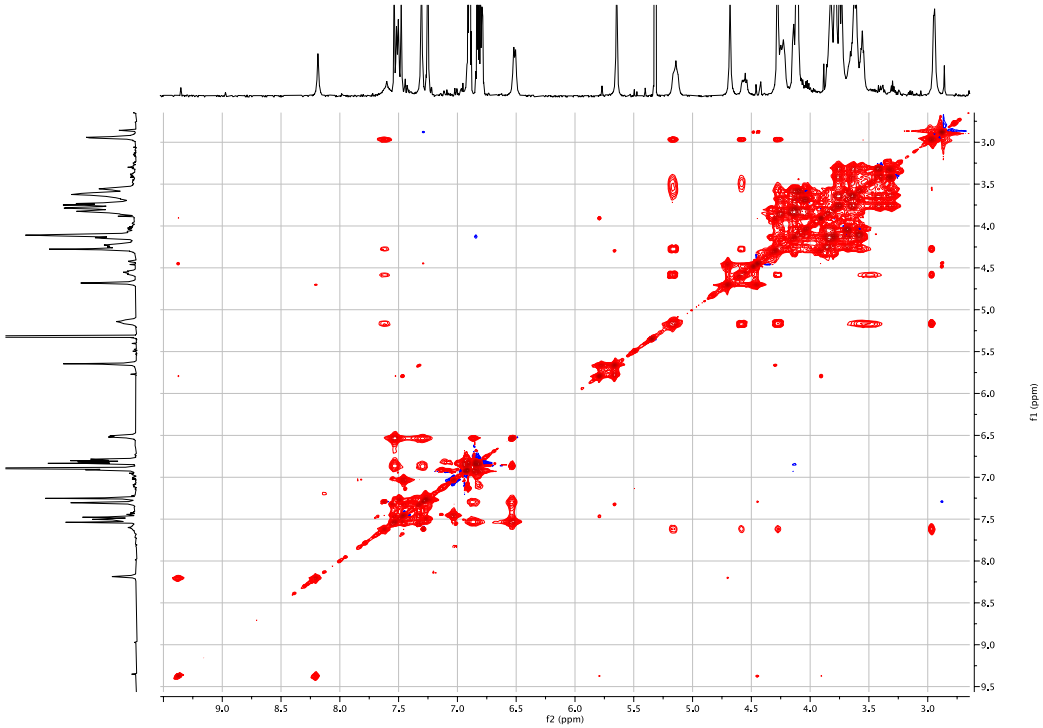

Figure S21. TOCSY spectrum of **1**H^{2+}·$2PF_6^-$ (500 MHz, CD_2Cl_2, 298 K, spinlock 80 ms).

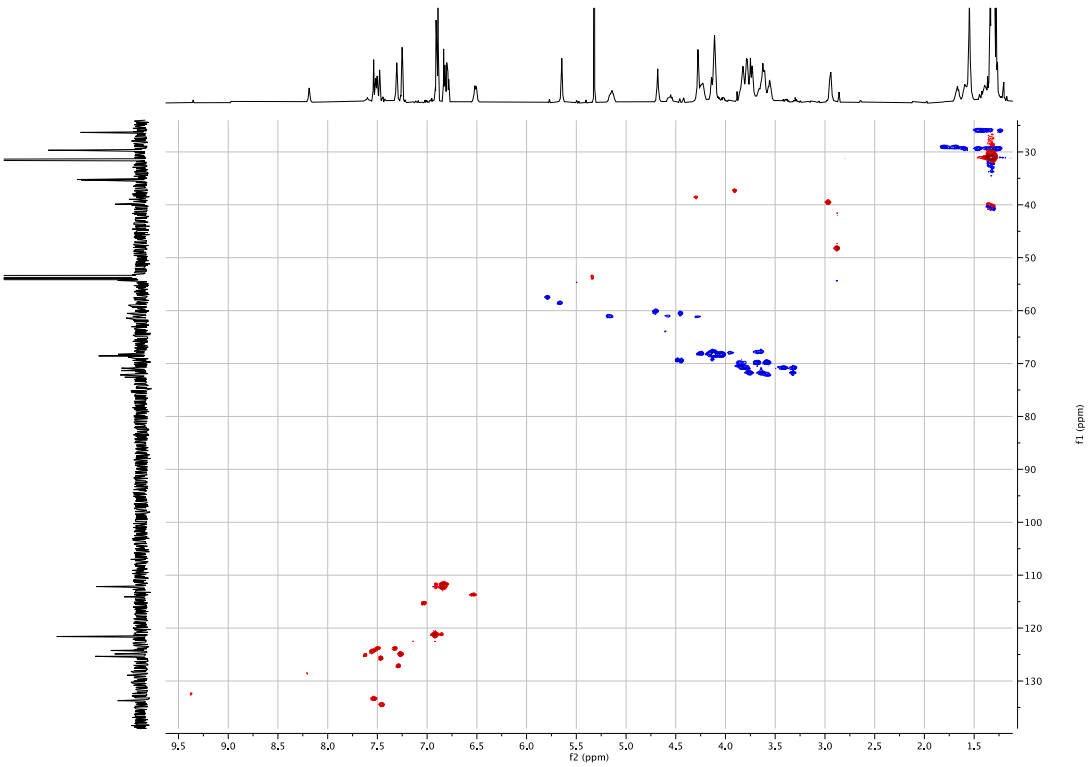

Figure S22. ^1H–^{13}C HSQC spectrum of **1**H^{2+}·$2PF_6^-$ (125 MHz, CD_2Cl_2, 298 K).

6. References

[1] M. Curcio, F. Nicoli, E. Paltrinieri, E. Fois, G. Tabacchi, L. Cavallo, S. Silvi, M. Baroncini and A. Credi, Chemically Induced Mismatch of Rings and Stations in [3]Rotaxanes. *J. Am. Chem. Soc.*, 2021, **143**, 8046–8055.

[2] D. Basak, S. Christensen, S. K. Surampudi, C. Versek, D. T. Toscano, M. T. Tuominen, R. C. Hayward and D. Venkataraman, Proton conduction in discotic mesogens. *Chem. Commun.*, 2011, **47**, 5566-5568

[3] J. M. Lehn, in Dynamic Stereochemistry. Fortschritte der Chemischen Forschung, Springer, Berlin, Heidelberg, 1970, vol 15/3 pp. 311–377.

[4] M. J. S. Dewar and W. B. Jennings, The Barrier to Pyramidal Inversion of Nitrogen in Dibenzylmethylamine. *J. Am. Chem. Soc.*, 1971, **93**, 401–403.

[5] M. W. Davies, M. Shipman, J. H. R. Tucker and T. R. Walsh, Control of Pyramidal Inversion Rates by Redox Switching. *J. Am. Chem. Soc.*, 2006, **128**, 14260–14261.

[6] S. Amano, S. D. P. Fielden and D. A. Leigh, A catalysis-driven artificial molecular pump. *Nature*, 2021, **594**, 529–534.